Dark matter distribution:

Standard halo (SH) model:

isothermal sphere with isotropic Maxwellian velocity distribution in Galactic rest-frame

$$f(\mathbf{v}) \propto \exp\left(-\frac{|\mathbf{v}|^2}{2\sigma^2}\right) \quad \text{for} \quad v < v_{\rm esc} \qquad \sigma = \frac{v_{\rm c}}{\sqrt{2}}$$

solution of collisionless Boltzmann equation with $\rho \propto r^{-2}$

standard parameter values:

local density		$\rho = 0.3\,{\rm GeV\,cm^{-3}}$
local circular speed		$v_{\rm c} = 220\,{\rm km\,s^{-1}}$
local escape speed	traditionally	$v_{\rm esc} = 650\,{\rm km\,s^{-1}}$
	more recently	$v_{\rm esc} = 554\,{\rm km\,s^{-1}}$ [RAVE]

RATE DIFERENCIAL

Si $v_{min} < v_{esc} - v_E$:

$$dR/dE_R = C\frac{k_0}{k_1}\frac{R_0}{E_0 r}(\frac{\sqrt{\pi}}{4}\frac{v_0}{v_E}(\text{erf}(\frac{v_{min}+v_E}{v_0}) - \text{erf}(\frac{v_{min}-v_E}{v_0})) - \exp(-\frac{v_{esc}^2}{v_0^2}))$$

Si $v_{min} < v_{esc} + v_E$:

$$dR/dE_R = C\frac{k_0}{k_1}\frac{R_0}{E_0 r}(\frac{\sqrt{\pi}}{4}\frac{v_0}{v_E}(\text{erf}(\frac{v_{esc}}{v_0}) - \text{erf}(\frac{v_{min}-v_E}{v_0})) - \frac{v_E+v_{esc}-v_{min}}{v_E/2}\exp(-\frac{v_{esc}^2}{v_0^2}))$$

$m_N = M_{DM}M_N/(M_{DM}+M_N)$

$m_n = M_{DM}M_n/(M_{DM}+M_n)$

$\sigma_N = \sigma_0\frac{m_N m_N}{m_n^2}A^2$

$k_0 = (\pi v_0^2)^{3/2}$

$k_1 = k_0(\text{erf}(v_{esc}/v_0) - \frac{2}{\sqrt{\pi}}\frac{v_{esc}}{v_0}\exp(-(v_{esc}/v_0)^2)$

$n_0 = \rho/M_{DM}$

$R_0 = \frac{2}{\sqrt{\pi}}\frac{N_0}{A}n_0 v_0 \sigma_N$

$E_0 = M_{DM}v_0^2/2.$

$r = 4M_{DM}M_N/(M_{DM}+M_N)^2$

$v_{min} = v_0\sqrt{\frac{E_R}{E_0 r}}$

$t = 0$ días desde el 1 de enero

$v_0 = 220$ km s^{-1}

$v_{esc} = 650$ km s^{-1}

$v_E = 244 + 15\cos(2\pi(t - 152.5)/365.25)$ km s^{-1}

$\rho = 0.3/c^2$ GeV c^{-2} cm^{-3}

$A = 28$ silicio

$M_N = 26.0603162/c^2$ GeV c^{-2}

$M_n = 0.938272/c^2$ GeV c^{-2}

$C = 8640 \cdot 1000$ conversión de unidades: [km cm GeV^{-1} s^{-1} g^{-1}] a [kg^{-1} día^{-1} keV^{-1}]

WIMP Signatures: Annual Modulation

Spectral function of WIMP rate: $$\frac{dR}{dE_R} = \frac{k_0}{k_1}\frac{R_0}{E_0 r}\left\{\frac{\sqrt{\pi}v_0}{4v_E}\left[erf\left(\frac{v_{min}+v_E}{v_0}\right) - erf\left(\frac{v_{min}-v_E}{v_0}\right)\right] - e^{-\frac{(v_{esc})^2}{v_0^2}}\right\}$$

- The velocity of the Earth varies over the year as the Earth moves around the Sun, and can be written as [in km/s]:

$$v_E(t) = v_0\left[1.05 + 0.07\cos\frac{2\pi(t-t_p)}{1yr}\right]$$

t = days since January 1st
t_p = 2. June (152.5 d) ± 1.3 d; 1 yr = 362.25 d

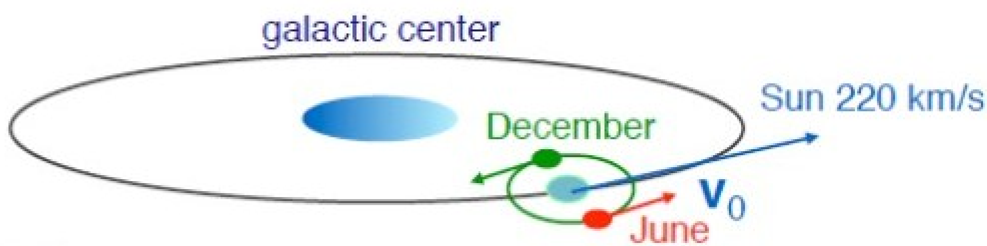

- the velocity modulation gives rise to a ~ 3% modulation in the rate $\frac{d}{dv_E}\left(\frac{R}{R_0}\right) \sim \frac{1}{2v_E}\frac{R}{R_0}$ (for $v_E \sim v_0$)

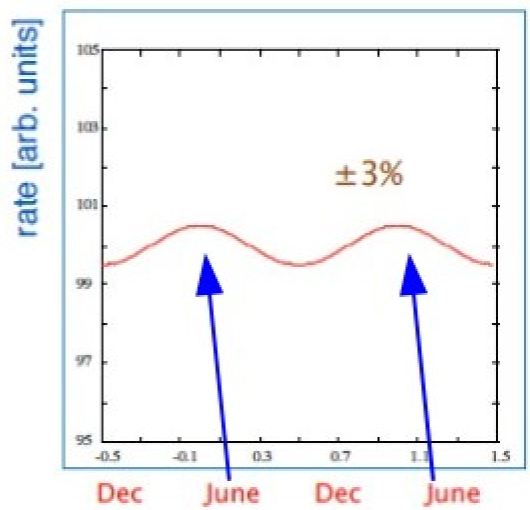

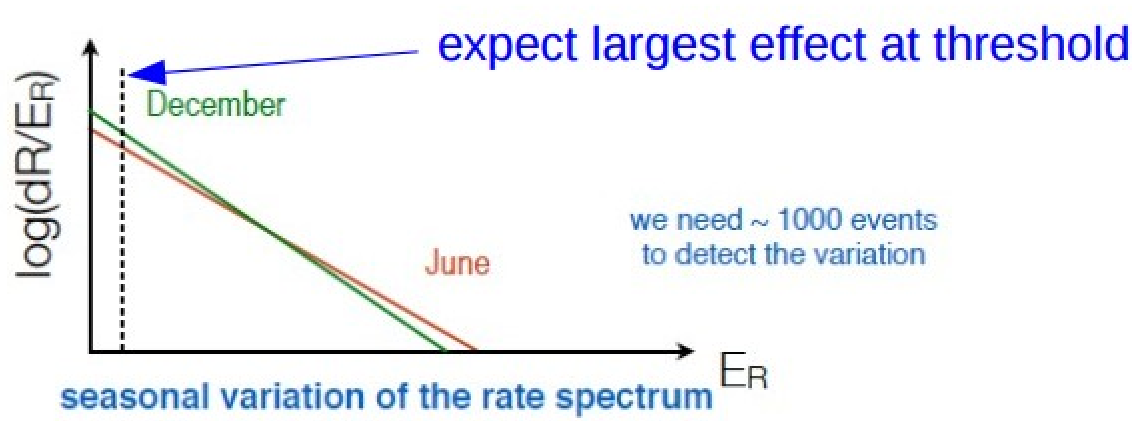

→ more faster WIMPs in June → more make it above threshold → higher rate

iii) annual modulation of event rate

Drukier, Freese & Spergel

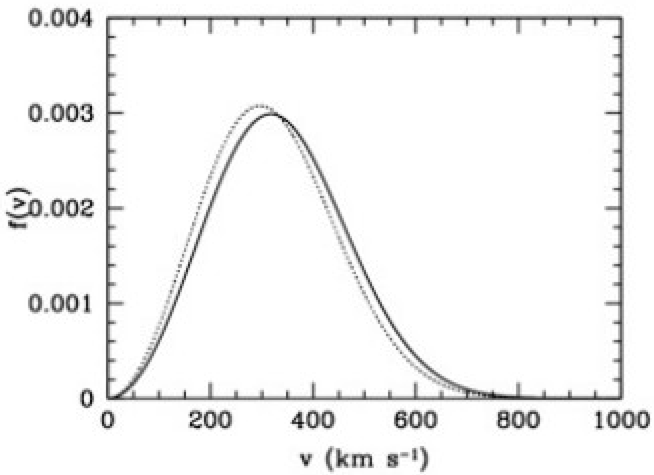

WIMP 'standard' (Maxwellian) speed dist.

detector rest frame (summer and winter)

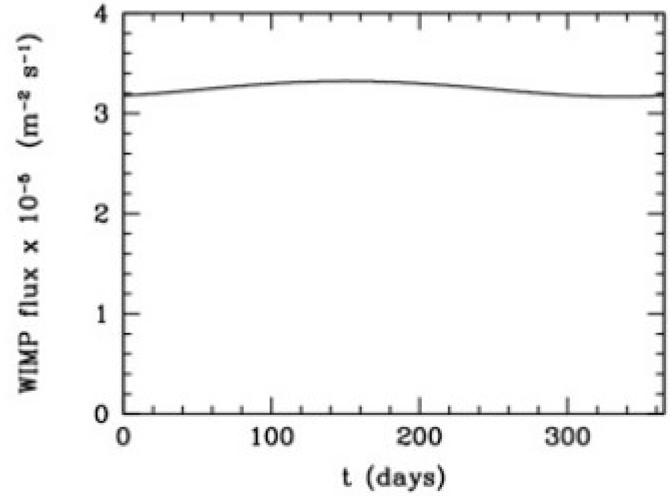

total WIMP flux

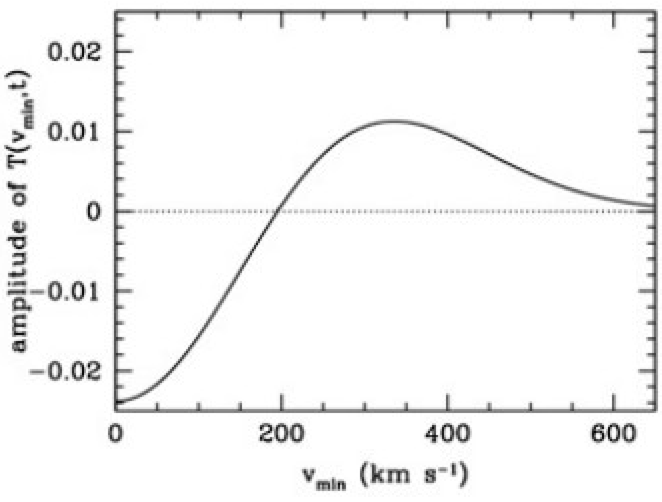

modulation amplitude

Signal O(few per-cent), therefore need large exposure.

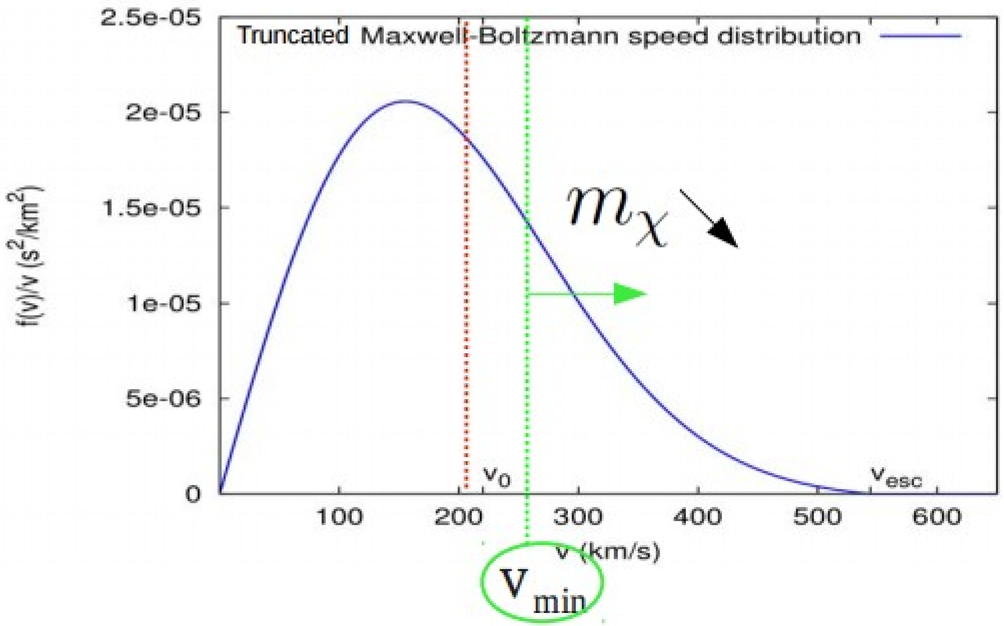

Truncated Maxwell-Boltzmann speed distribution
f(v)/v (s²/km²)
v (km/s)
v_0
v_{esc}
m_χ
V_{min}

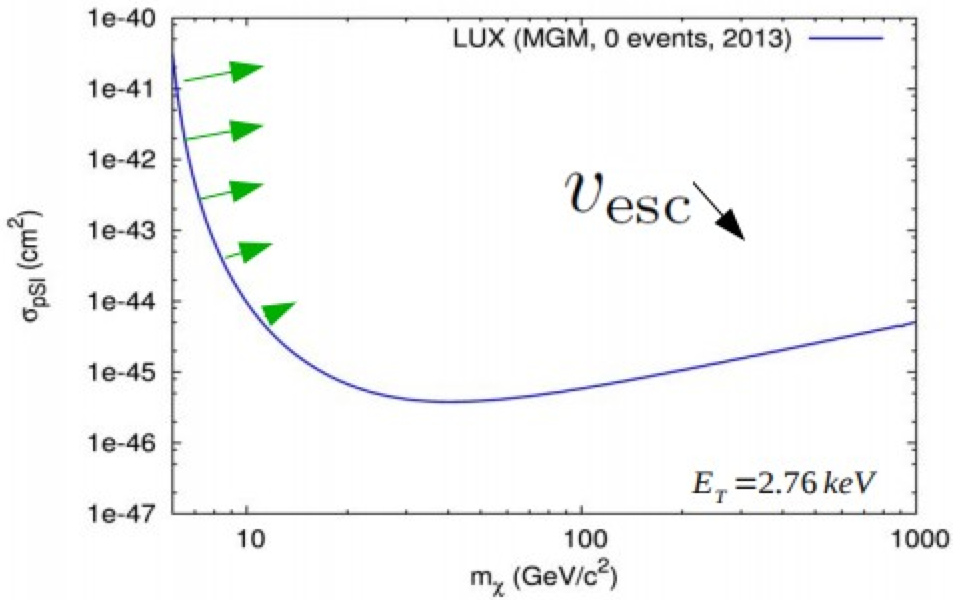

LUX (MGM, 0 events, 2013)
σ_{pSI} (cm²)
m_χ (GeV/c²)
v_{esc}
$E_T = 2.76\, keV$

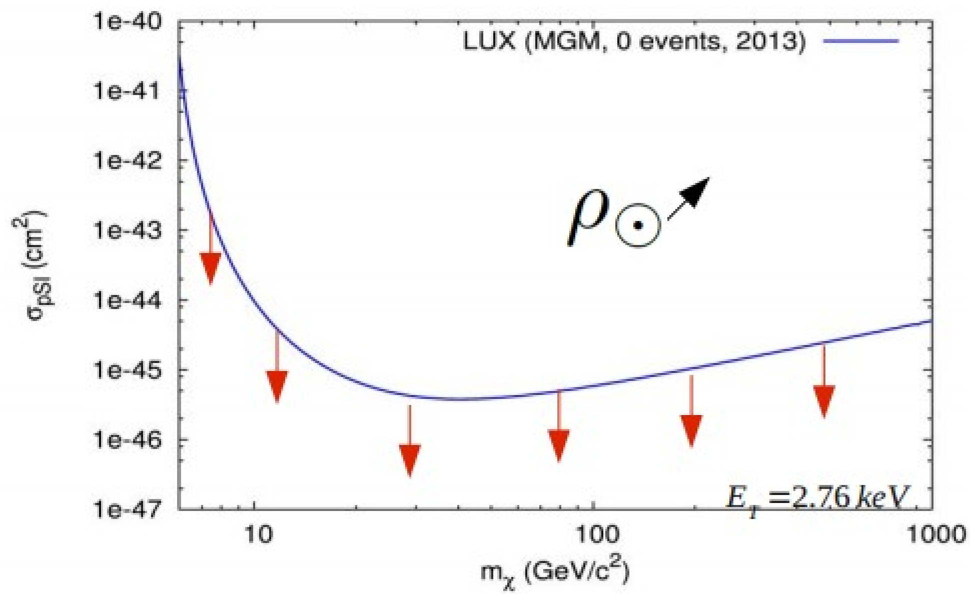

LUX (MGM, 0 events, 2013)
σ_{pSI} (cm²)
m_χ (GeV/c²)
$\rho_\odot$
$E_T = 2.76\, keV$

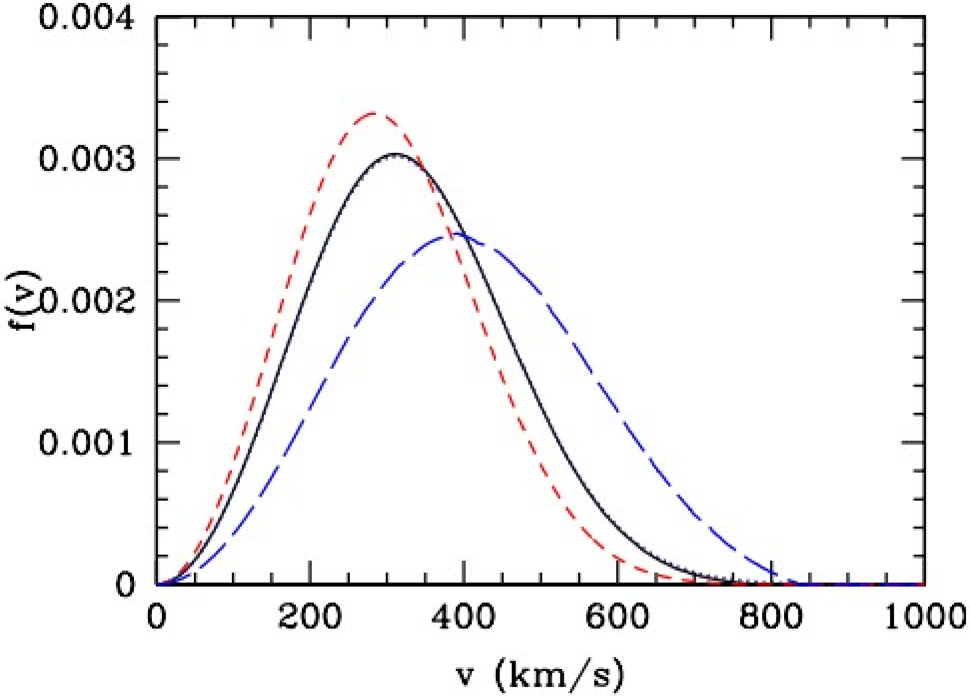

Normalised average speed distribution in the lab, SH with varying dispersion

———— (solid)	v_c = 220 km/s, v_{esc}=554 km/s
- - - - (red dashed)	200 km/s
— — — (blue long-dashed)	280 km/s
.... (green dotted)	220 km/s, v_{esc}=650 km/s

Simulations:

Vogelsberger et al.:

systematic deviations from multi-variate gaussian.

including high v features.

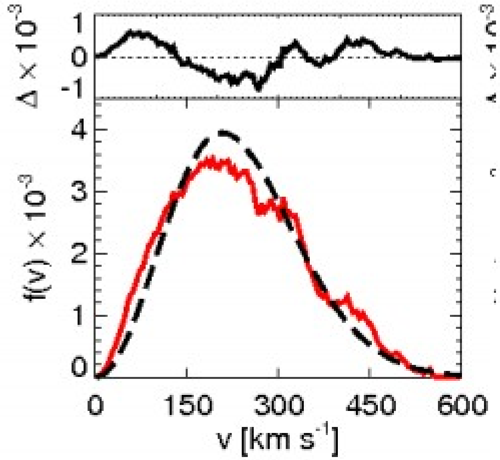

red lines: simulation data,
black lines: best fit multi-variate Gaussian

Hansen et al., Fairbairn & Schwetz and Kuhlen et al. have found similar results.

Modified Maxwellian distribution: $f(v_r) = \frac{1}{N_r} \exp\left[-\left(\frac{v_r}{\bar{v}_r}\right)^{\alpha_r}\right]$ $f(v_t) = \frac{v_t}{N_r} \exp\left[-\left(\frac{v_t}{\bar{v}_t}\right)^{\alpha_t}\right]$

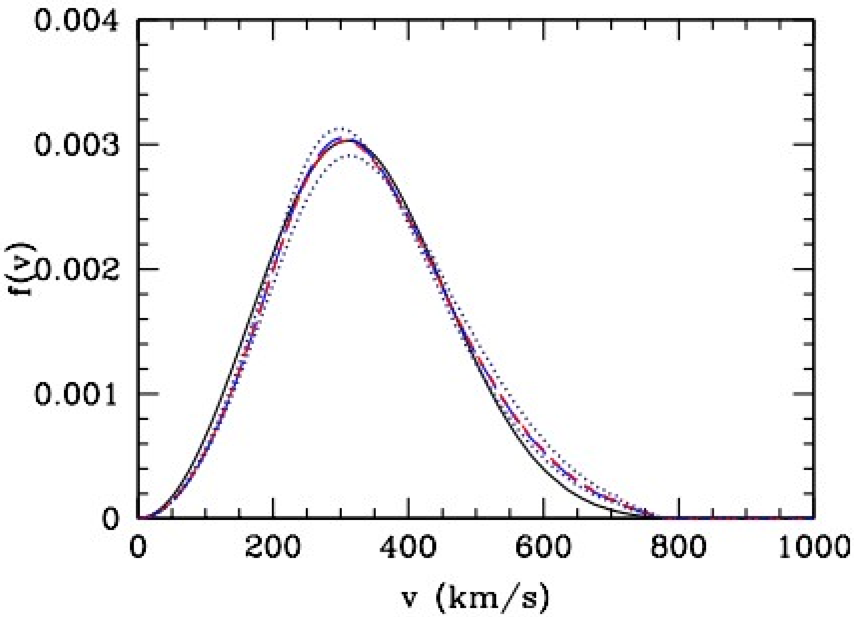

SH with same peak speed
fit to shell at solar radius
median fit to spheres at solar radius
spread in fits to spheres at solar radius

Caveats:

i) scales resolved by simulations are many orders of magnitude larger than those probed by direct detection experiments

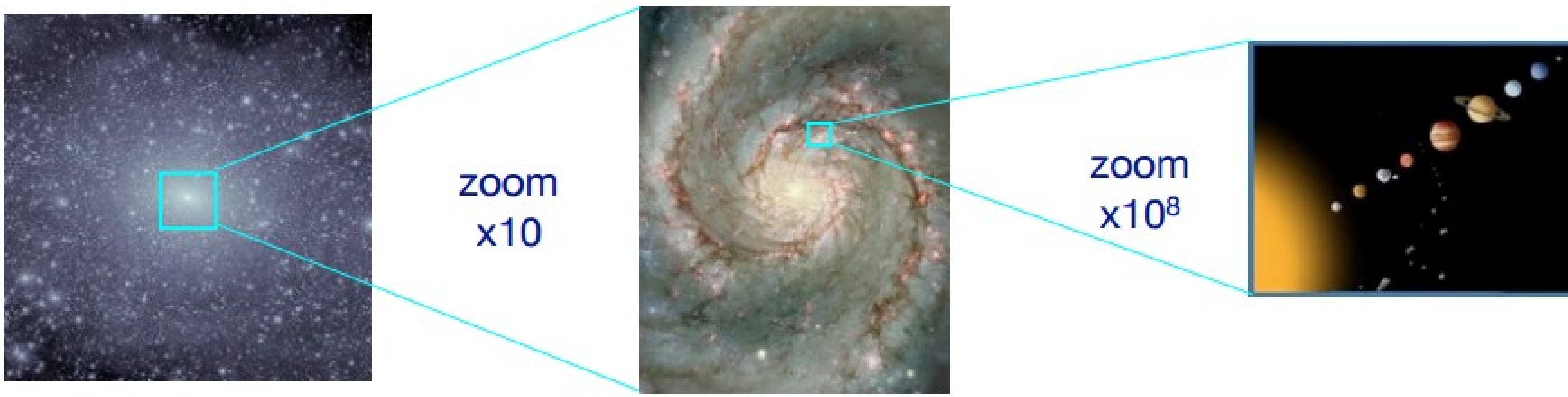

~300 kpc

~30 kpc

~0.3 mpc

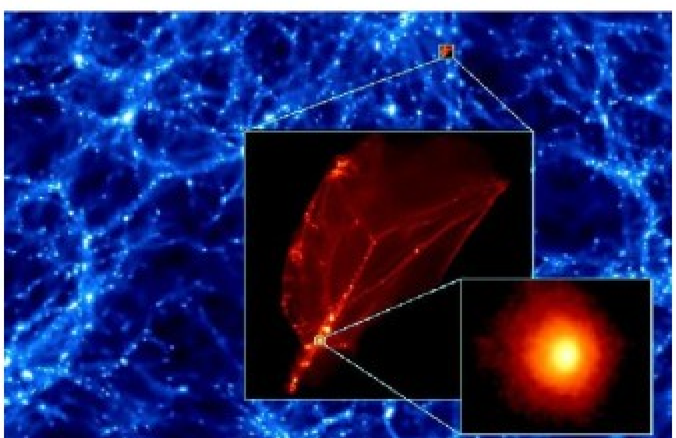

microhalo simulation
[Diemand, Moore & Stadel]

The first WIMP microhalos to form have

$M \sim 10^{-6} M_{\odot}$ [Green, Hofmann & Schwarz]

c.f. resolution of best Milky way simulations:

$M \sim 10^{5} M_{\odot}$

ii) effect of baryons on DM speed distribution?

Sub-halos merging at $z<1$ preferentially dragged towards disc, where they're destroyed leading to the formation of a co-rotating dark disc. Read et al, Bruch et al., Ling et al.

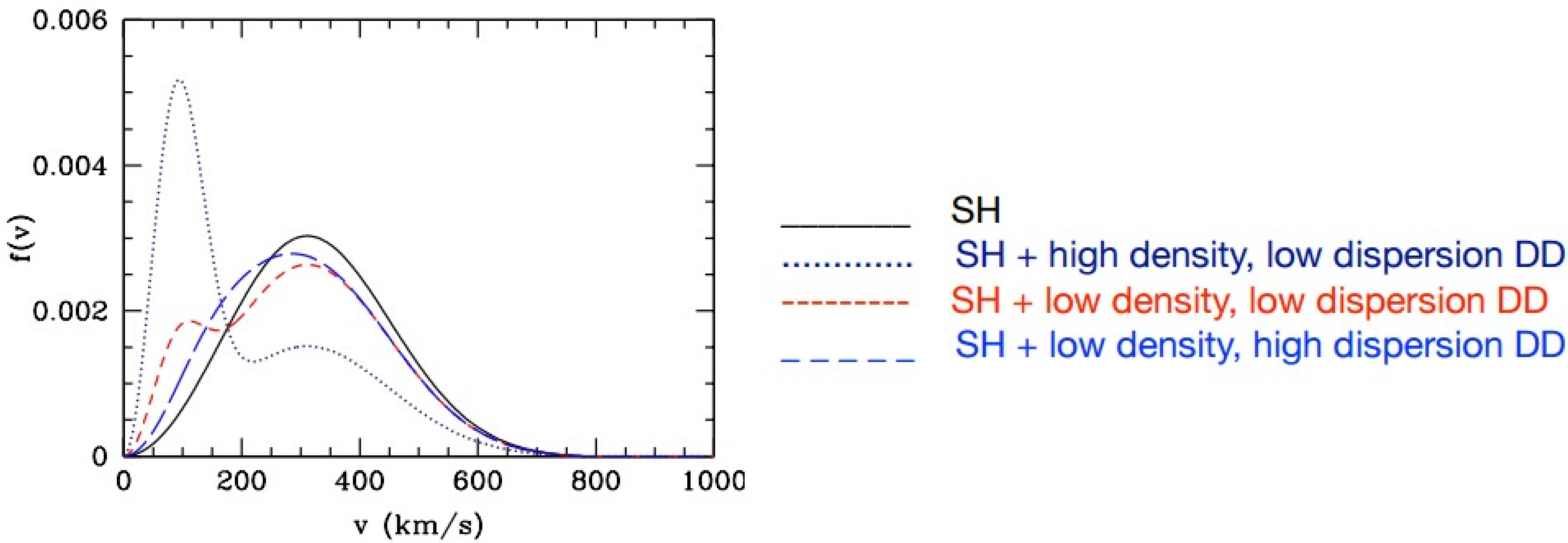

$$\mathcal{L}_{\text{int}} = \sum_{N=n,p} \sum_i c_i^{(N)} \mathcal{O}_i \chi^+ \chi^- N^+ N^-,$$

1. P-even, S_χ-independent

$$\mathcal{O}_1 = \mathbf{1}, \qquad \mathcal{O}_2 = (v^\perp)^2, \qquad \mathcal{O}_3 = i\vec{S}_N \cdot (\vec{q} \times \vec{v}^\perp),$$

2. P-even, S_χ-dependent

$$\mathcal{O}_4 = \vec{S}_\chi \cdot \vec{S}_N, \qquad \mathcal{O}_5 = i\vec{S}_\chi \cdot (\vec{q} \times \vec{v}^\perp), \qquad \mathcal{O}_6 = (\vec{S}_\chi \cdot \vec{q})(\vec{S}_N \cdot \vec{q}),$$

3. P-odd, S_χ-independent

$$\mathcal{O}_7 = \vec{S}_N \cdot \vec{v}^\perp,$$

4. P-odd, S_χ-dependent

$$\mathcal{O}_8 = \vec{S}_\chi \cdot \vec{v}^\perp, \qquad \mathcal{O}_9 = i\vec{S}_\chi \cdot (\vec{S}_N \times \vec{q})$$

5. P-odd, S_χ-independent:

$$\mathcal{O}_{10} = i\vec{S}_N \cdot \vec{q},$$

6. P-odd, S_χ-dependent

$$\mathcal{O}_{11} = i\vec{S}_\chi \cdot \vec{q}.$$

SI cross section

- Now have dependence on q^2 and nucleus → separate out fundamental WIMP-nucleon cross section
- Differential cross section can be written

$$\frac{d\sigma_{WN}(q)}{dq^2} = \frac{\sigma_{0WN}\, F^2(q)}{4m_r^2 v^2}$$

rel. velocity in CM frame

where σ_{0WN} is total cross section for $F = 1$.
From Fermi's Golden Rule

$$\frac{d\sigma_{WN}(q)}{dq^2} = \frac{1}{\pi v^2}|M|^2 = \frac{1}{\pi v^2} f_n^2 A^2 F^2(q)$$

- Can identify "unity-form-factor" cross sections:

$$\sigma_{0WN} = \frac{4m_r^2}{\pi} f_n^2 A^2 = \underbrace{\frac{4}{\pi} m_n^2 f_n^2}_{\sigma_{Wn}} \frac{m_r^2}{m_n^2} A^2$$

nucleus

nucleon

all the particle physics, here

Coherent Scatter Processes

Weakly Interacting Massive Particles

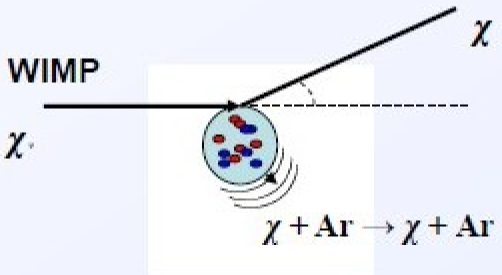

$$\lambda_{\text{300 Gev WIMP}} = \frac{h}{m \times v} = 5\,fm$$

$$R_{\text{Xe nucleus}} = 6\,fm$$

Neutrino-nucleus scattering

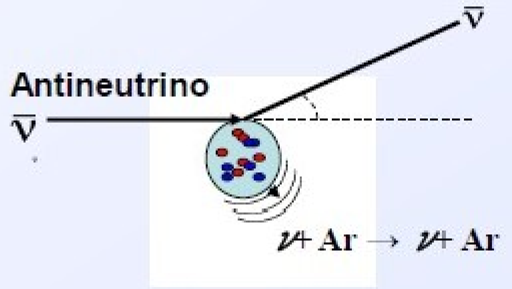

$$\lambda_{\text{reactor antineutrino}} = 300\,fm$$

$$R_{\text{Ar nucleus}} \sim 3\,fm$$

Both processes satisfy the coherence condition:

$$\lambda \geq R_{nucleus}$$

Nuclear form factor and Spin Ind. interactions

- Scattering amplitude: Born approximation $\vec{q} = \hbar\,(\vec{k}' - \vec{k})$
- Spin-independent scattering is coherent $\lambda = \hbar/q \sim \text{few fm}$

$$M(\vec{q}) = f_n\, A \underbrace{\int d^3x\, \rho(\vec{x})\, e^{i\,\vec{q}\cdot\vec{x}}}_{F(\vec{q})} \quad \Rightarrow \quad \sigma \propto |M|^2 \propto A^2$$

fundamental coupling to nucleon

mass number

"Helm" form factor

$$F(qr_n) = \underbrace{\frac{3[\sin(qr_n) - qr_n\cos(qr_n)]}{(qr_n)^3}}_{j_1(qr_n)}\, e^{-(qs)^2/2}$$

- j_1 exact for 'sharp' density cutoff
  - r_n nuclear radius
  - s skin thickness parameter

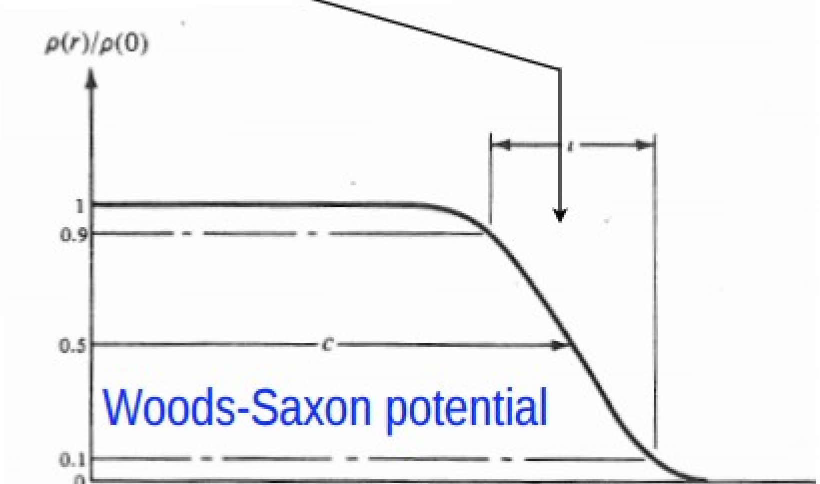

swiped from Fraunfelder and Henley

Nuclear form factor and Spin Ind. interactions

- Loss of coherence as larger momentum transfer probes smaller scales

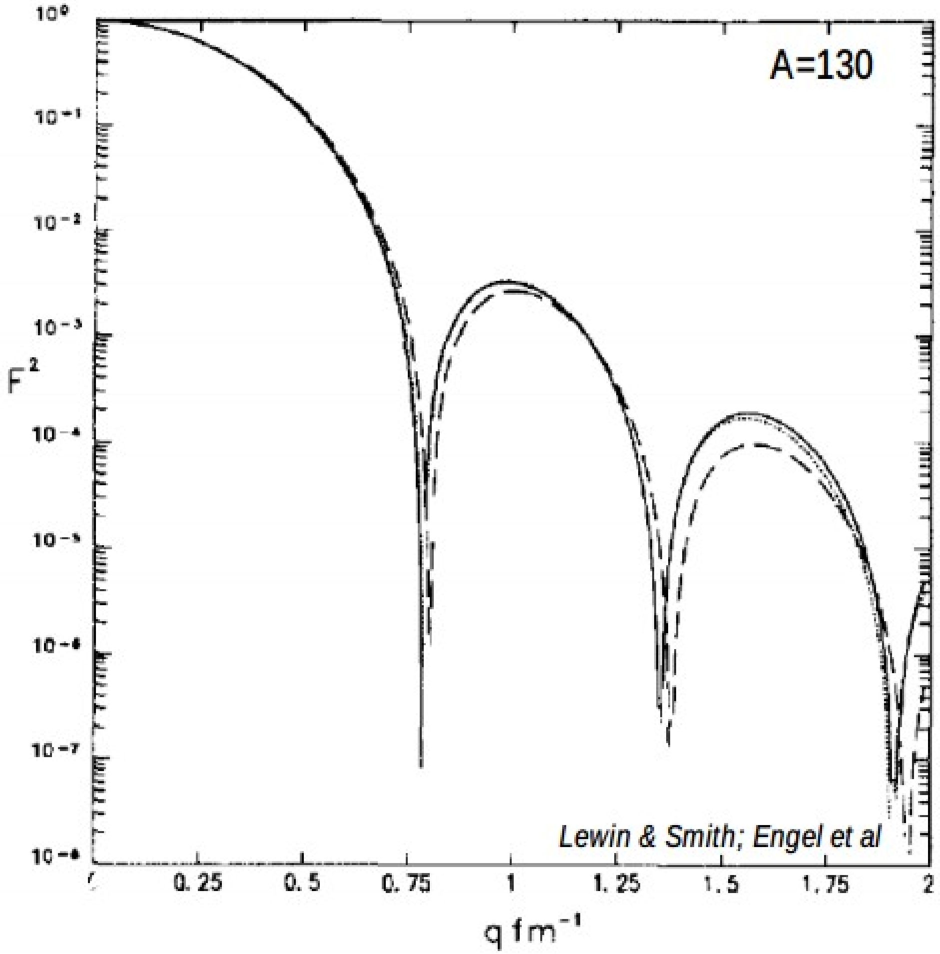

Signal Quenching

WIMPs (and neutrons) scatter off nuclei
→ nuclear recoils
γ and β backgrounds scatter off electrons
→ electronic recoils

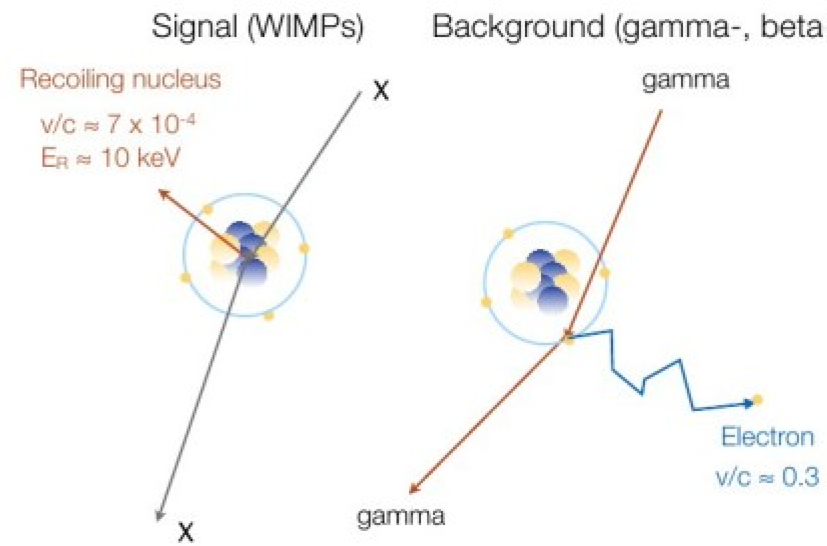

Detectors respond differently to both types of recoils since the energy loss mechanisms are weigthed differently:

$$\left(\frac{dE}{dx}\right)_{tot} = \left(\frac{dE}{dx}\right)_{elec} + \left(\frac{dE}{dx}\right)_{nucl}$$

Ionization, excitation — heat

In the regime of low nuclear Er, the nuclear stopping power plays a significant role
→ less ionization and excitation of target atoms
→ less observed signal in ionization/scintillation detectors
→ Signal Quenching („Lindhard theory")

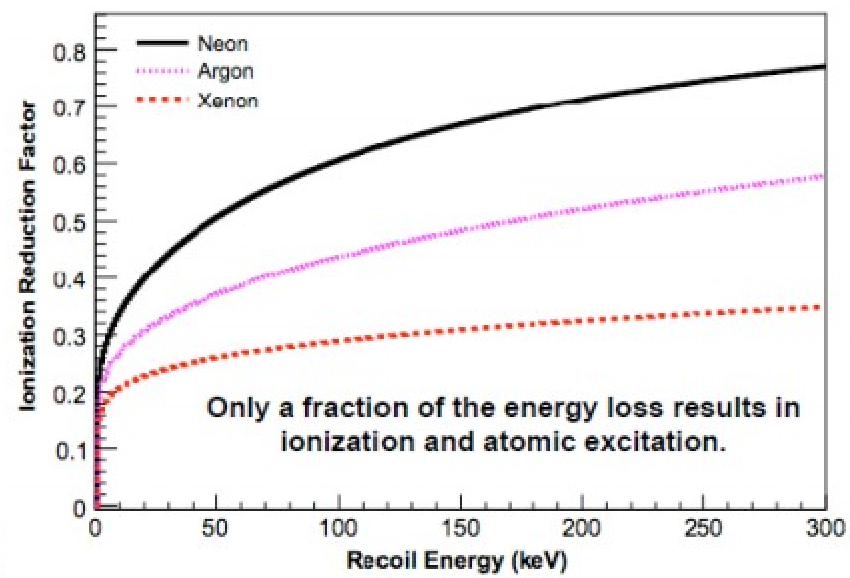

In addition to this, there might be other effects which lead to quenching, e.g. bi-excitonic quenching in LXe
(higher ionization density from NRs impacts the generation of scintillation light)